Autoreduction of a six-coordinate Fe(III)TPP–peroxide complex by heterolytic iron–oxygen bond cleavage

Kunihiko Tajima*, Kohichi Mikami, Kohji Tada, Shigenori Oka**, Kazuhiko Ishizu
Department of Chemistry, Faculty of Science, Ehime University, Matsuyama 790 (Japan)

and Hiroaki Ohya-Nishiguchi
Department of Chemistry, Faculty of Science, Kyoto University, Kyoto 606 (Japan)

(Received September 3, 1991; revised November 25, 1991)

Abstract

ESR, optical and NMR measurements have been carried out to study the reactions occurring between Fe(III)TPP($^-OCH_3$)$_2$ (complex **A**) and t- or n-butylhydroperoxide in DMSO. The addition of t- or n-BHPO to complex **A**, in aerobic conditions, caused a marked shift of the absorption maxima, and resulted in the disappearance of the ESR signal due to the formation of diamagnetic species. The observed optical spectrum of the new iron complex (complex **B**) is explained as the Fe(II)TPP($^-OCH_3$)$_2$ species. In addition, the results of NMR measurements justified that complex **B** takes the ferrous low-spin state ($S=0$). The presence of an intermediate species (complex **C**), in the reduction processes of complex **A** to **B**, was demonstrated by means of simultaneous ESR and optical measurements, combined with the rapid mixing and freezing treatment. From comparison of the optical and ESR parameters of complex **C** and related iron complexes, the complex was ascribed to be six-coordinate Fe(III)TPP($^-OCH_3$)($^-$OO-butyl), in which the deprotonated peroxide anion binds at the axial position. After standing the reaction mixture at 298 K for about 1 min, the ESR signal due to complex **C** disappeared, and an identical optical spectrum to complex **B** was observed. This means that the Fe(III)TPP–peroxide complex can be reduced to complex **B**, in which it is in the ferrous low-spin state. Based on these observation results, a possible reaction mechanism for autoreduction of complex **C** will be discussed.

Introduction

It has been well established that several heme enzymes, such as cytochrome P-450 [1] and tryptophan di-oxygenase [2], exhibit oxygenation activity toward substrate molecules utilizing molecular oxygen. Based on the distinct behavior of the manner of oxygenation, these two enzymes were classified into mono- and di-oxygenases, respectively. The P-450 enzyme catalyzes insertion of an oxygen atom into a wide variety of organic substrates when coupled with an NADPH containing reductase [3]. The reductase plays an important role in conversion of the P-450–oxygen complex to the corresponding P-450–peroxide adduct. The peroxide complex is believed to be further activated by either homolytic or heterolytic cleavage occurring at the oxygen–oxygen bond of the peroxide moiety. The bond cleavage results in formation of the high valent iron complexes, so called compound **I** and **II**, which are expected to be the essentially important intermediate species in the mono-oxygenation processes of P-450. On the other hand, TDO promotes the di-oxygenation of tryptophan to the formylkinurenin derivatives, in which two oxygen atoms derived from atmospheric oxygen are involved. In the reaction pathway of TDO, the formation of the TDO–oxygen–substrate ternary complex [4] has been assumed to be the transient intermediate species. Both oxygen atoms of the complex were thought to be directly inserted into the substrate molecule, followed by cleavage occurring at the iron–oxygen bond. The bond cleavage reactions occurring not only at the oxygen–oxygen bond, but also at the iron–oxygen bond, have been presumed to be the key reaction stage for the mono- and di-oxygenases.

In the last decade, oxygen–oxygen bond cleavage of heme–peroxide complexes has been extensively studied by using synthetic iron porphyrin complexes. Groves and Watanabe [5] for example, have reported the formation of compound **I** species from the five-coordinate iron porphyrin–acylperoxide complex. In addition, LaMar and co-workers [6] have demonstrated the formation of compound **II** species by thermal decom-

*Author to whom correspondence should be addressed.
**Present address, Kyoto Pharmaceutical University, Yamashina-ku, Kyoto 607, Japan.

0020-1693/92/$5.00

position of the Fe(III)TPP–μ-oxodimer complex at 248 K. The chemical reactivity of these high-valent iron complexes towards substrate molecules were also studied with relation to the homo-oxygenation action of P-450 [7]. On the contrary, mechanistic investigations on iron–oxygen bond cleavage reactions have been scarcely reported.

Recently, we [8] have reported a possible model reaction system of TDO, composed of Fe(III)TPP, 3-methyl-indole, molecular oxygen and alkaline reagent. The results of products analyses demonstrated that 3-methyl-indole was catalytically oxygenated to *o*-formamidoacetophenon (*o*-FA), in which two oxygen atoms derived from atmospheric oxygen were involved. By means of simultaneous ESR and optical measurements, the formation of a transient intermediate species, taking the ferric low-spin state, was detected. Comparison of the optical and ESR parameters of the complex and related ferric low-spin species, suggested that the complex was a six-coordinate Fe(III)TPP-organic peroxide complex [9–11]. Based on the positive detection of $^{17}O_2$ splittings in the g_3 component of the observed ESR spectrum, the axially ligating peroxide moiety was assumed to be the deprotonated form of 3-hydroperoxo-3-methyl-indolenin. Such a complex should be a practical chemical model for the heme–oxygen–substrate ternary complex assumed in the reaction cycle of TDO.

Using the assumption that the ternary complex of TDO can be a six-coordinate heme–organic peroxide complex, we have started investigations on the chemical reactivity of the peroxide complex, focusing upon the iron–oxygen bond cleavage reaction. The reaction between Fe(III)TPP and t- or n-butylperoxide (t- or n-BHPO) in the presence of an alkaline reagent was studied in the same manner. We found that the aerobic addition of t- or n-BHPO to a DMSO solution of the Fe(III)TPP($^-OCH_3$)$_2$ complex resulted in the generation of a ESR non-detectable iron complex. On the basis of the observed optical and ^{1}H NMR properties, the complex was assumed to be the six-coordinate ferrous low-spin complex ($S=0$). The simultaneous ESR and optical measurements, coupled with the rapid mixing and freezing method, demonstrated the presence of the ferric low-spin species ($g_1=2.312$, $g_2=2.155$ and $g_3=1.955$; λ_{max} 430, 538 and 681 nm), as an intermediate species. The observed ESR and optical property of the complex was consistent with those of Fe(III)TPP–peroxide complexes [10]. These findings suggest that the Fe(III)TPP–peroxide complex is spontaneously reduced to the ferrous low-spin species followed by heterolytic cleavage of the iron–oxygen bond. In this report, the possible reaction mechanisms for the autoreduction of the Fe(III)TPP–peroxide complex will be discussed.

Experimental

Materials

The free base of $TPPH_2$ [12] and its iron complex Fe(III)TPPCl were prepared by the usual procedures described by Adler *et al.* [13]. The purity of Fe(III)TPPCl was checked by elemental analysis and NMR. tert-Butylhydroperoxide (t-BHPO) was obtained from Nakarai Tesque Co. Ltd., and was used after distillation twice under reduced pressure. n-Butylhydroperoxide [14] was prepared and purified in our laboratory according to the ordinary methods. The concentration of a methanol solution of sodium methoxide was calibrated by pH titrations. DMSO was used after drying (CaH_2) and distillation before each measurement.

Measurements

Optical absorption spectra at 77 K were recorded by using an Ohtsuka Electronic Co. Ltd., MCPD-100 spectrophotometer, with wavelength range from 400 to 800 nm. Optical absorption spectra at 298 K were observed by a JASCO UVDEC-1 spectrometer with 0.1 mm flow optical cell. ESR spectra were usually measured at 77 K, and 4.2 K as required, by a JEOL FE2XG X-band spectrometer operating with 100 kHz field modulation. The microwave frequency applied to the sample (5.0 mW) was monitored by an Advantest TR-5212 digital frequency counter. The magnetic field strength was calibrated by the hyperfine coupling constant (86.9 gauss) of the Mn(II) ion doped in MgO powder. The g values of the observed ESR spectra were estimated based on the g value of the Li–TCNQ radical salt ($g=2.0025$) as a standard. ^{1}H NMR spectra were recorded in DMSO-d_6 using a JEOL GX-270 (270 MHz) spectrometer at 298 K. All measurements were performed at the Advantest Instrumental Center for Chemical Analysis, Ehime University.

Results and discussion

Reaction between Fe(III)TPP and peroxide under alkaline conditions

As shown in Fig. 1(a), a DMSO solution of Fe(III)TPPCl (1.0 mM, 0.4 ml) gave absorption maxima at 416, 497, 529 and 689 nm, as featured by a broad Soret band absorption maximum. The frozen solution gave the ESR signals at $g_\perp=6$ and $g_\parallel=2$ (Fig. 2(a)), which are typical of the porphyrin iron complex of the ferric high-spin ($S=5/2$) state [15]. The observed optical and ESR parameters of the complex were consistent with those reported for the six-coordinate Fe(III)TPP(DMSO)$_2$ complex (Table 1) [16], in which two DMSO molecules bind at both axial positions. Then a methanol solution of sodium methoxide (0.75 M,

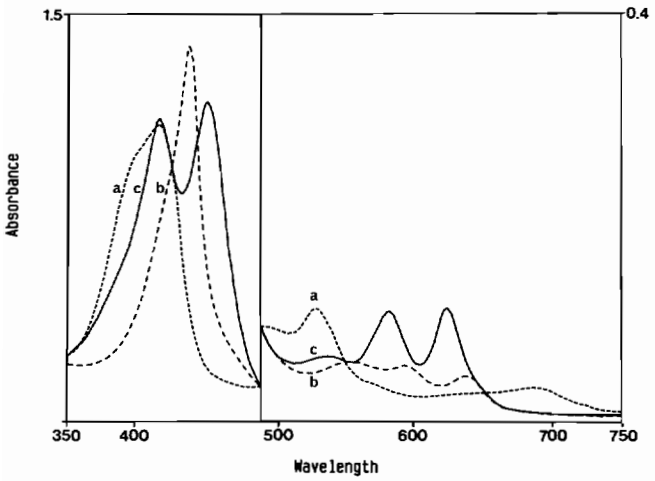

Fig. 1. Optical absorption spectra recorded at 298 K: (a) spectrum observed for DMSO solution of Fe(III)TPPCl (0.5 mM, 0.4 ml); (b) spectrum observed after addition of sodium methoxide methanol solution (0.75 M, 0.012 ml); mixing molar ratio of Fe(III)TPP:sodium methoxide is 1:45; methanol content is 3.0%; (c) spectrum observed after addition of n-BHPO (1.0 M, 0.02 ml) to the reaction mixture of (b) at 298 K; mixing molar ratio of Fe(III)TPP:n-BHPO is 1:60.

Fig. 2. ESR spectra observed at 77 K for the same reaction solution supplied for optical measurements at 298 K (Fig. 1(a) to (c)): (a) ESR spectrum observed for DMSO solution of Fe(III)TPPCl (0.5 mM, 0.4 ml); (b) ESR spectrum observed after addition of sodium methoxide methanol solution (0.75 M, 0.012 ml); (c) spectrum observed after addition of n-BHPO (1.0 M, 0.02 ml) to the reaction mixture of (b) at 298 K.

0.012 ml) was added to the reaction mixture. The molar ratio of Fe(III)TPPCl and methoxide was 1:45 and the methanol content was fixed at 3.0%. As shown in Fig. 1(b)), the absorption maxima were shifted to 436, 549, 594 and 638 nm, respectively. The ESR spectrum (Fig. 2(b)) observed for the reaction mixture revealed the formation of the ferric low-spin complex (denoted as complex **A**; $g_1 = 1.915$, $g_2 = 2{,}163$ and $g_3 = 2.484$) with strong signal intensity. The formation of complex **A** arose from an axial ligand exchange reaction occurring between the DMSO molecules and the methoxide anion derived from the alkaline reagents. In fact, the observed optical and ESR parameters of complex **A** agreed well with those of Fe(III)TPP($^-OCH_3$)$_2$ complexes [10, 16, 17] recorded in several organic solvents (Table 1). The Fe(III)TPP($^-OCH_3$)$_2$ species (complex **A**) was confirmed to be the predominant species existing in the dry DMSO solution composed of Fe(III)TPPCl and sodium methoxide.

Reactions occurring between complex **A** and t- or n-butylhydroperoxide (t- and n-BHPO) were monitored by optical absorption and ESR spectroscopy. As shown in Fig. 2(c), the ESR signal intensity due to complex **A** was markedly depressed by addition of n-BHPO (1.0 M, 0.02 ml), and a new ESR signal of the free radical species (denoted as R) was observed at $g = 2.01$. The three weak ESR signals ($g_1 = 1.96, g_2 = 2.16$ and $g_3 = 2.31$) were detected whenever n-BHPO was added to complex **A**. The accurate coordination structure and the chemical reactivity of the paramagnetic species will be discussed in the following. A weak ESR signal of a non-heme iron complex was also observed in the lower magnetic field at $g = 4.3$. This means that small amounts of non-heme by-products from the oxidative decomposition of Fe(III)TPPCl were formed in the presence of butylhydroperoxide [9, 10]. Other paramagnetic iron species were not detected for the same frozen solution even at 4.2 K. The optical spectrum recorded after addition of n-BHPO revealed the split Soret band at 414 and 448 nm, with the Q band absorption maxima at 563, 577 and 626 nm (Fig. 1(c)). The presence of the four isosbestic points at 425, 486, 549 and 653 nm suggested that the Fe(III)TPP($^-OCH_3$)$_2$ complex in solution is changed to a new absorbing species (denoted as complex **B**) on reaction with n-BHPO. The same reaction mixture was used for optical measurement at 77 K. As shown in Fig. 3, the observed optical spectrum showed a distinctively different line shape, as featured by the Soret band and a pair of Q-band absorption maxima at 425, 530 and 561 nm. This suggests that the optical spectrum of complex **B** can be changed depending upon the observation temperature.

With the same mixing molar ratio, the ESR signal due to complex **A** was also quenched on addition of t-BHPO to a solution of complex **A**. In this case, the ESR signal of the t-butyl peroxide radical was clearly detected at $g_{\parallel} = 2.033$ and $g_{\perp} = 2.008$ values, which are consistent with the g value of the t-butylperoxide radical derived from t-BHPO [22]. The formation of complex **B** was also demonstrated by optical absorption measurements at 298 and 77 K, as summarized in Table 1. By comparison with the optical parameters of complex

TABLE 1. ESR[a] and optical property of six-coordinate ferric and ferrous low-spin complexes

Complex	Solvent	Base	Peroxide	Temperature[b] (K)	λ_{max} (nm)[c]	g_1	g_2	g_3	Reference
Fe(III)TPP(DMSO)$_2$	DMSO	none	none	298	416 497 529 689	($g=6$, $g=2$)			[m]
Fe(III)TPP(DMSO)$_2$	DMSO	none	none	298	415 497 530 687	($g=6$, $g=2$)			16
Complex **A**	DMSO	S[d]	none	298	436 549 594 638	1.915	2.163	2.484	[m]
Fe(III)TPP($^-$OCH$_3$)$_2$	DMSO	S	none	298	436 550 595 640	1.914	2.165	2.442	16
Fe(III)TPP($^-$OCH$_3$)$_2$	CH_2Cl_2	S	none	77	430 546 588 652	1.921	2.166	2.497	10
Fe(III)TPP($^-$OCH$_3$)$_2$	CH_2Cl_2	choline	none	77	430 546 586 654	1.921	2.166	2.497	10
Complex **B**	DMSO	S	t-BHPO	298	414 448 536 577 626	diamagnetic			[m]
Complex **B**	DMSO	S	n-BHPO	298	414 448 535 577 620	diamagnetic			[m]
Complex **B**	DMSO	S	t-BHPO	77	425 530 561	diamagnetic			[m]
Complex **B**	DMSO	S	n-BHPO	77	425 530 561	diamagnetic			[m]
Complex **B**	DMSO[e]	S	t-BHPO	77	425 530 561	diamagnetic			[m]
Complex **B**	DMSO[e]	S	n-BHPO	77	425 530 561	diamagnetic			[m]
Fe(II)TPP($^-$OCH$_3$)$_2$[f]	DMSO	S	none	298	417 450 535 580 622	diamagnetic			16
Fe(II)TPP(pip)$_2$[g]	toluene	none	none	298	422 530 561	diamagnetic			18
Fe(II)TPP-(Im)$_2$[h]	DMF	none	none	298	427 533 566	diamagnetic			19
Fe(II)TPP-(py)$_2$[i]	CH_2Cl_2	none	none	298	528 561	diamagnetic			20
Complex **C**	DMSO	S	t-BHPO	77	423 538 581	1.955	2.155	2.316	[m]
Complex **C**	DMSO	S	n-BHPO	77	423 538 581	1.945	2.163	2.323	[m]
Complex **C**	DMF	S	t-BHPO			1.952	2.160	2.320	[m]
Complex **C**	DMF	S	n-BHPO			1.948	2.162	2.324	[m]
Complex **C**	toluene	S	t-BHPO			1.956	2.162	2.324	[m]
Complex **C**	toluene	S	n-BHPO			1.956	2.160	2.325	[m]
Complex **C**	CH_2Cl_2	S	t-BHPO			1.952	2.160	2.323	[m]
Complex **C**	CH_2Cl_2	S	n-BHPO			1.949	2.607	2.316	[m]
Fe(III)TPP($^-$OCH$_3$)-($^-$OO-butyl)	CH_2Cl_2	S	t-BHPO	77	420 543 571	1.952	2.157	316	10
Fe(III)TPP($^-$OCH$_3$)-($^-$OO-butyl)	CH_2Cl_2	TBAOH	t-BHPO	77	420 543 573	1.953	2.154	2.316	10
Fe(III)TPP($^-$OCH$_3$)-($^-$OO-butyl)	CH_2Cl_2	choline	t-BHPO	77	420 544 573	1.955	2.154	2.316	10
Fe(III)TPP($^-$OCH$_3$)-($^-$OO-skatole)[j]	CH_2Cl_2	S	t-BHPO	193	422 548 587	1.951	2.170	2.316	8
Fe(III)TPP($^-$OCH$_3$)-($^-$OO-skatole)[j]	CH_2Cl_2	TMAOH[k]	t-BHPO	193	421 550 586	1.952	2.169	2.316	8
Fe(III)TPP($^-$OCH$_3$)-($^-$OO-LHPO)$_l$	CH_2Cl_2	choline	LHPO$_l$			1.933	2.172	2.332	21

[a]ESR spectra were recorded at 77 K. [b]Temperature of optical measurements. [c]Experimental error in Soret band 77 K is within ± 8 nm. [d]S, sodium methoxide. [e]Prepared from complex **C** by thaw and freezing treatment at 25 °C. [f]Observed under nitrogen atmosphere. [g]pip, piperidine. [h]Im, imidazole. [i]py, pyridine. [j]skatole, 3-methylindole. [k]TMAOH, tetramethylammonium hydroxide. [l]LHPO, linolenic acid hydroperoxide. [m]Present work.

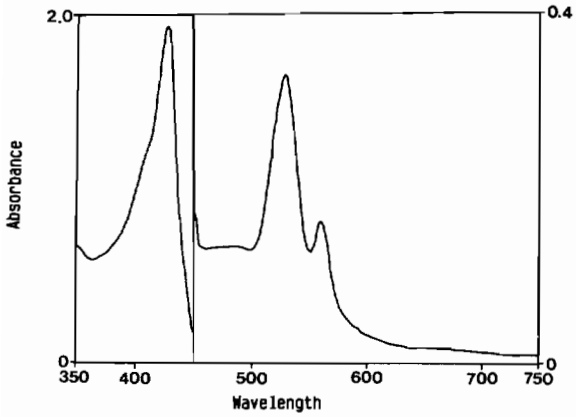

Fig. 3. Optical absorption spectrum recorded at 77 K for the frozen mixture containing complex **B**, prepared by addition of n-BHPO (1.0 M, 0.02 ml) to complex **A** at 298 K.

B prepared by n- and t-BHPO, the molecular structure of butylperoxide was thought to be independent of the optical property of complex **B**. These results obtained from the optical and ESR measurements demonstrated that complex **A** was changed to an ESR non-detectable iron complex **B** by reaction with t- or n-BHPO.

The observed optical property of complex **B** measured at 298 and 77 K were compared with the numerical optical parameters of Fe(II)TPP and Fe(III)TPP complexes already reported. The observed absorption maxima of complex **B** at 77 K were analogous to those of the six-coordinate Fe(II)TPP species, such as Fe(II)TPP–$(Im)_2$ [18] and –$(piperidine)_2$ [19] complexes, taking the ferrous low-spin state, as summarized in Table 1. The values of the absorption maxima of complex **B** showed excellent agreement with those of Fe(II)TPP$(py)_2$ [20] within experimental error (Table 1). By comparison of the optical parameters of complex **B** with related ferrous complexes, the coordination structure of complex **B** at 77 K was assumed to be the six-coordinate low-spin ($S=0$) Fe(II)TPP$(^-OCH_3)_2$ complex. This observation result was consistent with the results of ESR measurements which suggested that complex **B** is an ESR non-detectable iron complex even at 4.2 K. The optical parameters of complex **B** observed at 298 K were consistent with those of the Fe(II)TPP$(^-OCH_3)_2$ species [16], prepared in dry DMSO containing sodium methoxide (Table 1). The complicated optical spectrum of the complex has been assumed to be the mixture of Fe(II)TPP$(^-OCH_3)_2$ species and its protonated form. However, the accurate electronic structure of complex **B** at 298 K is still equivocal.

With the aid of ^1H NMR spectroscopy, further efforts were made to clarify the spin state of complex **B** at 298 K. The DMSO-d_6 solution of complex **B** was prepared by addition of n- or t-BHPO and methanol-d_4 solution of $NaOCD_3$ to Fe(III)TPPCl with the same mixing molar ratio. As shown in Fig. 4, NMR signals due to the porphyrin moiety of complex **B** were detected at 8.5 and 7.17 ppm, and no significant NMR signal was observed in the lower and higher magnetic field. Therefore, a paramagnetic iron complex, such as a ferrous high-spin ($S=4/2$) complex [23] can be safely ruled out for complex **B** at 298 K. As summarized in Table 2, the observed NMR chemical shift of complex **B** (8.5 and 7.17 ppm) showed excellent accordance with those of ferrous low-spin complexes [23–25]. Furthermore, the integrated intensity of the signals detected at 8.5 and about 7.17 ppm were estimated to be 8:20, which agreed with the ratio of pyrrole (8*H*) and phenyl protons (20*H*) of the Fe(II)TPP complex. Combining the results obtained from NMR and optical measurements, the electronic structure of complex **B** is also confirmed to be the ferrous low-spin state ($S=0$) at 298 K, as well as at 77 K. This finding indicates that complex **A** is reduced by one-electron to complex **B**, which exists in the low-spin ferrous state.

Complex **B** was fairly stable towards oxygen, while the excess amounts of t- or n-BHPO remained in the reaction mixture. There was no significant spectral change for complex **B**, when standing the solution for about 1 h under ambient condition. Formation of complex **B** was not detected in the absence of butyl peroxides, under aerobic conditions. Sodium methoxide was also indispensable in generating complex **B** by reaction with butyl peroxide. Of interest is the fact that the content of methanol in DMSO also affected the reaction between complex **A** and t- or n-BHPO. When the methanol content exceeded 20%, generation of complex **B** was not complete, and absorption maxima due to complex **A** were still observed. This means that the presence of excess amounts methanol disturb the formation of complex **B**. In addition, the formation of complex **B** was also inhibited in water containing DMSO, no matter how the methanol content was adjusted, at 3.0%. These observations indicate that a proton source, such as methanol and water, disturbs the formation of complex **B**.

Detection of intermediate complex existing in the process of complex B formation

Three weak ESR signals ($g_1=1.96$, $g_2=2.16$ and $g_3=2.31$ (Fig. 2(c)) were detected by addition of t- or n-BHPO to complex **A**. Based on the ESR line-shape of these signals, the paramagnetic species was thought to be the ferric low-spin species. However, the ESR signal intensity was too weak for the detailed coordination structure to be deduced. In order to obtain informations about the structure of the species, simultaneous ESR and optical measurements were continued with the aid of the rapid mixing and freezing methods [10]. With the same mixing molar ratio as

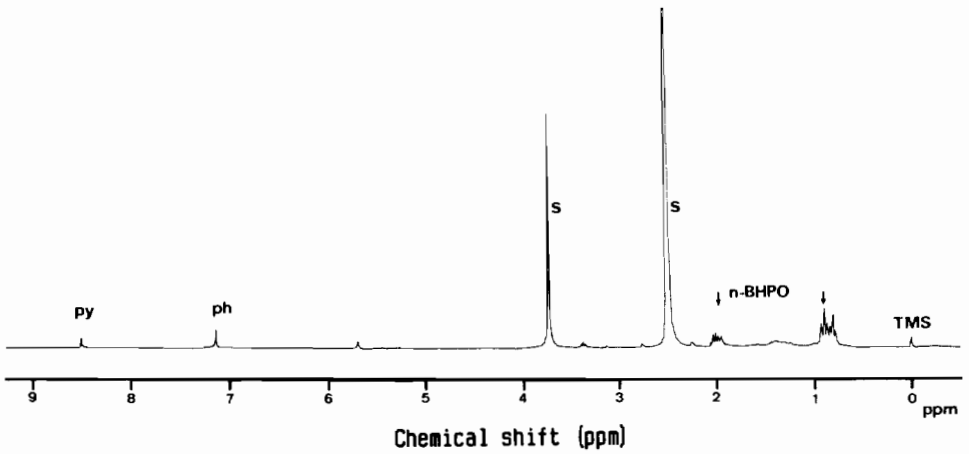

Fig. 4. NMR spectrum observed at 298 K for the DMSO solution of complex **B** prepared after addition of n-BHPO to complex **A** at 298 K under aerobic condition. Abbreviations: py, pyrrole protons of complex **B**; ph, phenyl ring protons of complex **B**; S, NMR signal due to solvent protons; n-BHPO, NMR signal ascribed to n-BHPO protons; TMS, tetramethylsilane.

TABLE 2. ^{1}H NMR parameters (ppm) of the ferrous low-spin Fe(II)TPP complexes

Complex	Solvent	Temperature	Pyrrol	Phenyl	Reference
Complex **B**	DMSO-d_6	298	8.5	7.17	[a]
Fe(II)TPP(pip)$_2$[b]	CD_2Cl_2	195	8.0	7.97, 7.56, 7.33	18
Fe(II)TPP(CO)	toluene	300	8.9	7.5, 8.1	24
Fe(II)TPP($^-$CN)$_2$	DMSO-d_6	298	7.9	7.64, 7.65, 7.60	25

[a]Present work. [b]pip, piperidine.

described above, the DMSO solution of t-BHPO was rapidly added to complex **A**, and the resulting solution was immediately frozen at 77 K within about 5 s. Color of the frozen solution changed to bright red after addition of butyl peroxide. The optical absorption spectrum recorded at 77 K gave the Q-band absorption maxima at 538 and 581 nm, as shown in Fig. 5. The ESR spectrum (Fig. 6) revealed formation of the ferric low-spin complex (denoted as complex **C**; $g_1 = 1.955$, $g_2 = 2.155$ and $g_3 = 2.316$), while the ESR signal intensity due to complex **A** was markedly diminished. The free radical species of the t-butylperoxide radical was also detected at $g_{\parallel} = 2.033$ and $g_{\perp} = 2.008$. Similar optical and ESR spectra ascribable to complex **C** were also observed when n-BHPO was added to complex **A** but the same procedures. The ESR and optical parameters of complex **C** prepared by t- and n-BHPO showed excellent agreement within experimental error (Table 1). The observed g parameters of complex **C** are consistent with that of the weak three ESR signals ($g_1 = 1.96$, $g_2 = 2.16$ and $g_2 = 2.31$).

Recently, analogous ESR and optical spectra to those of complex **C** have been observed for frozen dichloromethane solution containing six-coordinate Fe(III)TPP-butylperoxide complexes [10]. Based on the ESR spectrometric titration, the possible coordination structure of the complex was assumed to be Fe(III)TPP($^-$OCH$_3$)($^-$OO-t-butyl). By comparison of g values of complex **C** and of relating Fe(III)TPP–butylperoxide complexes (Table 2), complex **C** was safely classified as the six-coordinate Fe(III)TPP–peroxide complex. Furthermore, a resemblance was also recognized between the optical parameters of complex **C** and of the peroxide complex, as summarized in Table 2. Thus complex **C** is proposed to be the six-coordinate Fe(III)TPP($^-$OCH$_3$)($^-$OO-t- or -n-butyl) complex, in which the deprotonated peroxide anion binds at the axial position.

The chemical reactivity of complex **C** was studied by means of the thaw and freeze treatments [9, 26, 27]. The frozen DMSO solution of complex **C** prepared by using t-BHPO was thawed once at 298 K for about 1 min, then ESR and optical spectra were again recorded. As shown in Fig. 6(b), the ESR signal due to complex **C** almost disappeared, on the contrary, the ESR signal intensity due to the t-butyl peroxide radical

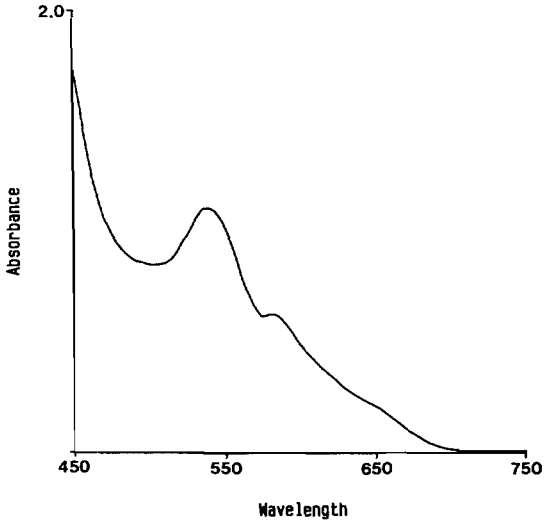

Fig. 5. Optical absorption spectrum recorded as 77 K for the frozen solution prepared by rapid mixing and freezing method; DMSO solution of t-BHPO (0.5 M, 0.04 ml) was rapidly added to the solution composed of Fe(III)TPPCl (0.5 mM, 0.4 ml) and sodium methoxide methanol solution (0.75 M, 0.012 ml), and the resulting mixture was immediately frozen at 77 K within about 5 s.

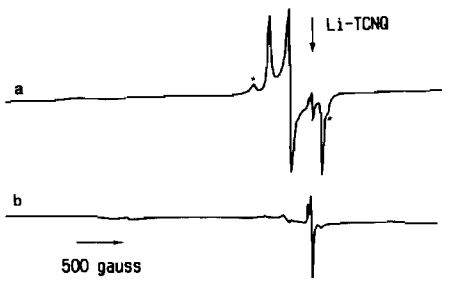

Fig. 6. ESR spectrum observed for complex C at 77 K. (a) ESR spectrum recorded for the same frozen solution supplied for optical measurements at 77 K (Fig. 5); (b) ESR spectrum recorded after the thaw and freezing treatment at 298 K for about 3 min. Asterisks are ESR signals due to the g_1 and g_3 components of complex A.

increased after the thaw and freezing treatment. The same frozen solution gave an optical spectrum as characterized by absorption maxima at 425, 530 and 561 nm, which agreed well with the optical property of complex **B** at 77 K (Table 1). The peroxide complex **C**, prepared by using n-BHPO, was also converted to complex **B** by the thaw and freezing treatment. These observations justified the fact that complex **C** had very short lifetime at 298 K, and was spontaneously autoreduced to complex **B** within about 1 min. Therefore, complex **C** is confirmed to be one of the intermediate species involved in the present autoreduction processes, as illustrated in Scheme 1.

Similar reactions between Fe(III)TPPCl and t- or n-BHPO in the presence of sodium methoxide were

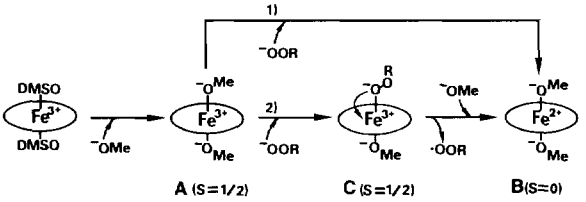

Scheme 1. Possible mechanisms for the reaction between Fe(III)TPPCl and t- or n-BHPO in the presence of sodium methoxide: (1) reaction between complex A and t- or n-BHPO at 298 K under aerobic condition; (2) the rapid mixing and freezing treatment of complex A and b- or n-BHPO. Abbreviations: ⁻OMe, the methoxide anion; ⁻OOR, the deprotonated form of t- and n-BHPO; ·OOR, the t- or n-butyl peroxide radical; the allow of complex C means the intramolecular one-electron transfer occurring from the peroxide anion to the iron chromophore.

studied in several organic solvents, such as dichloromethane, toluene and DMF. Formation of the Fe(III)TPP–peroxide complex was successfully detected by ESR. As summarized in Table 1, the observed ESR parameters were comparable with those recorded for complex **C** in DMSO. The solvent effect on the chemical reactivity of complex **C** was also investigated by monitoring the ESR signal intensity of complex **C**. However, complex **C** prepared in these organic solvents was readily decomposed to the non-heme iron complex ($g=4.3$) [9, 10] after standing the solution of complex **C** at 298 K for about 3 min. In addition, the formation of complex **B** was never detected in these organic solvents. These observations indicated that the oxidative denaturation of complex **C** precedes the formation of complex **B**, in dichloromethane, toluene and DMF. Thus DMSO is confirmed to be the unique solvent supporting the one-electron reduction of complex **C** to complex **B**. By comparison of the dielectronic constants (D) [28] of DMSO (48.9) and dichloromethane (9.08), toluene (2.37) and DMF (36.7), we find that DMSO possesses the highest D value of the organic solvents used. Solvation of the DMSO molecule to butyl peroxide anions is expected to be one of the important factors for the reduction of complex **C**, in the present reaction system.

Probable mechanism for the autoreduction of peroxide complex C

The reduction process of the ferric iron complex, so called autoreduction [29], has frequently been recognized for six-coordinate Fe(III)TPP complexes, in which the axial positions of heme are occupied by strong donors such as piperidine [20], $^-OCH_3$ [16] and CN^- anion [25]. Gaudio and LaMar [18], for example, reported that the Fe(III)TPP(piperidine)$_2$ complex was autoreduced to the corresponding ferrous low-spin complex. Based on the NMR and ESR study, the reducing agent of the reaction is identified as the piperidine molecule binding at the axial positions of Fe(III)TPP.

In addition, Sato and co-workers [16] have also reported that the Fe(III)TPP($^{-}OCH_3$)$_2$ complex, prepared in DMSO with low methanol concentration, was also autoreduced to Fe(II)TPP species. In this case, strict de-gas of DMSO would be required for the autoreduction of the Fe(III)TPP complex to proceed. This is the reason why the reoxidation of the Fe(II)TPP species proceeded rapidly to yield the Fe(III)TPP complex when the solution was exposed to air. In contrast, the ferrous complex **B** was fairly stable under an oxygen atmosphere, as mentioned above. This provides important evidence that a certain reductant could be involved in the reaction system. Taking into account the fact that complex **C** is an intermediate species, the axially ligating peroxide anion of complex **C** is expected to be the most probable candidate for the reducing agent. Followed by the intramolecular one-electron transfer, occurring from the peroxide anion to the iron chromophore, the axially binding peroxide anion would be eliminated as the peroxide radical. In fact, the peroxide radical species was clearly detected by ESR spectroscopy (Fig. 6(b)) during the thaw and freezing treatment of complex **C**. On the other hand, the one-electron reduced iron chromophore is assumed to be converted to complex **B**, after the re-binding of the methoxide anion at the axial position. Therefore, the heterolysis of the iron–oxygen bond of complex **C** is expected to be the important reaction stage in the autoreduction process of complex **C**, as is schematically illustrated in Scheme 1. To our present knowledge, the autoreduction of complex **C** is the first example of heterolytic bond cleavage occurring at the iron–oxygen bond of the peroxide complex.

So far, the chemical reactivity of heme–peroxide complexes, such as alkylperoxide [9–11], hydrogen peroxide [30] and fatty acid peroxide [21] have been studied by spectroscopic methods. These peroxide complexes provided important information about the heterolysis and homolysis of the oxygen–oxygen bond of the peroxide moiety [7]. However, the reaction mechanisms of the iron–oxygen bond cleavage were still obscure, in spite of the important relation to the oxygen activation processes of tryptophan dioxygenase. The present results demonstrate that the six-coordinate Fe(III)TPP–butyl peroxide complex **C** was autoreduced to the ferrous low-spin complex **B** in DMSO, after heterolysis of the iron–oxygen bond. The findings described here provide experimental evidence that the peroxide anion potentially exhibits reduction activity towards the iron chromophore in an aprotic polar solvent. Further investigations, to understand the reason why complex **C** prepared in DMSO is autoreduced to complex **B**, are now in progress.

Acknowledgements

The authors express their sincere thanks to Professor Dr Hiromu Sakurai of Kyoto Pharmaceutical University and Dr Kiyoko Yamamoto of the Institute of Physical and Chemical Research. The authors are also indebted to Dr Hiroyuki Tani of the Advanced Instrumental Center for Chemical Analysis, Ehime University for his kind help in NMR measurements. This work was partially supported by a Grant-in-Aid for Scientific Research from the Ministry of Education, Science and Culture, Japan.

References

1 I. C. Gunsalus and S. Sliger, *Adv. Enzymol. Relat. Areas Mol. Biol., 47* (1978) 1; V. Ullrich, *Top. Curr. Chem., 83* (1972) 67.
2 O. Hayaishi, S. Rothberg, A. H. Mehler and Y. Saito, *J. Biol. Chem., 229* (1957) 889; W. N. Poillon, H. Maeno, M. Koike and P. Feugelson, *J. Biol. Chem., 244* (1972) 3447; O. Hayaishi, in T. E. King, H. Mason and M. Morrison (eds.), *Oxidases and Related Redox Systems,* Pergamon, New York, 1982, p. 787.
3 R. E. White and M. J. Coon, *Ann. Rev. Biochem., 49* (1980) 315.
4 Y. Ishimura, M. Nozaki, O. Hayaishi, T. Nakamura and I. Yamazaki, *J. Biol. Chem., 245* (1970) 3593.
5 J. T. Groves and Y. Watanabe, *Inorg. Chem., 26* (1987) 785.
6 D.-H. Chin, G. N. LaMar and A. L. Balch, *J. Am. Chem. Soc., 102* (1980) 1446; *102,* (1980) 5946.
7 J. T. Groves, R. C. Haushalter, M. Nakamura and T. E. Nemo, *J. Am. Chem. Soc., 103* (1981) 1884; K. Shin and H. M. Goff, *J. Am. Chem. Soc., 109* (1987) 3140; T. G. Traylor and F. Xu, *J. Am. Chem. Soc., 112* (1990) 178; T. C. Bruice, C. M. Dicken, F. Lu and M. W. Nee, *J. Am. Chem. Soc., 107* (1985) 5776; M. J. Gunter and P. Turner, *Coord. Chem. Rev., 108* (1991) 115.
8 K. Tajima, M. Yoshino, K. Mikami, T. Edo, K. Ishizu and K. Ishizu, *Inorg. Chim. Acta, 172* (1990) 83; K. Tajima, *Chem. Chem. Ind., 44* (1991) 110.
9 K. Tajima, K. Ishizu, H. Sakurai and H. Ohya-Nishiguchi, *Biochem. Biophys. Res. Commun., 135* (1986) 972.
10 K. Tajima, J. Jinno, K. Ishizu, H. Sakurai and H. Ohya-Nishiguchi, *Inorg. Chem., 28* (1989) 709.
11 K. Tajima, *Inorg. Chim. Acta, 169* (1990) 211.
12 D. A. Adler, F. R. Longo, J. D. Finarelli, J. Goldmacher, J. Assour and L. Korsakoff, *J. Org. Chem., 32* (1967) 476.
13 A. D. Adler, F. R. Longo and V. Vardi, *Inorg. Synth., 16* (1976) 213.
14 H. R. Williams and H. S. Mosher, *J. Am. Chem. Soc., 76* (1954) 2984.
15 G. Palmer, in D. Dolphin (ed.), *The Porphyrins,* Vol. 4, Academic Press, New York, 1979, p. 313.
16 T. Ohtsuka, T. Ohya and M. Sato, *Inorg. Chem., 24* (1985) 776.
17 T. Ohtsuka, T. Ohya and M. Sato, *Inorg. Chem., 23* (1984) 1777.
18 D. Gaudio and G. N. LaMar, *J. Am. Chem. Soc., 100* (1978) 1112.

19 J. Mispelter and D. Lexa, *Biochem. Biophys. Acta, 338* (1974) 151.
20 D. L. Andersson, C. J. Weschler and F. Basolo, *J. Am. Chem. Soc., 96* (1974) 5599.
21 K. Tajima, M. Shigematsu, J. Jinno, Y. Kawano, K. Mikami, K. Ishizu and H. Ohya-Nishiguchi, *Biochem. Biophys. Res. Commun., 166* (1990) 924.
22 S. Schlik and W. Chamulitrat, *J. Phys. Chem., 89* (1985) 4278.
23 G. N. LaMar and F. A. Walker, in D. Dolphin (ed.), *The Porphyrins,* Vol. 4, Academic Press, New York, 1979, p. 61.
24 H. M. Goff and S. Shirazi, *J. Am. Chem. Soc., 104* (1982) 6318.
25 D. W. Dixon, M. Barbush and A. Shirzi, *Inorg. Chem., 24* (1985) 1081.
26 K. Tajima, M. Sakamoto, K. Okada, K. Mukai, K. Ishizu, H. Sakurai and H. Mori, *Biochem. Biophys. Res. Commun., 115* (1983) 1002.
27 J. Jinno, M. Shigematsu, K. Tajima, H. Sakurai, H. Ohya-Nishiguchi and K. Ishizu, *Biochem. Biophys. Res. Commun., 176* (1991) 675.
28 A. Weissberger and E. P. Proskaner (eds.), *Organic Solvents,* Interscience, New York, 1955.
29 S. Sano *et al., Proc. Natl. Acad. Sci. U.S.A., 83* (1986) 531.
30 K. Tajima, *Inorg. Chim. Acta, 163* (1989) 115; K. Tajima, M. Shigematsu, J. Jinno, K. Ishizu and H. Ohya-Nishiguchi, *J. Chem. Soc., Chem. Commun.,* (1990) 144.